Resource-Efficient Technologies 3 (2019) 20–25

TOMSK POLYTECHNIC UNIVERSITY

Resource-Efficient Technologies

journal homepage: http://ojs.tpu.ru/index.php/res-eff

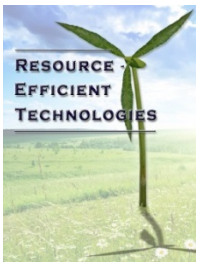

Research Paper

INVESTIGATION OF PULSE SHAPE NEUTRON-GAMMA DISCRIMINATION

R.V. Avetisyan*, R.H. Avagyan, A.E. Avetisyan, A.V. Gyurjinyan, A.G. Barseghyan, I.A. Kerobyan, A.A. Manukyan

A. Alikhanyan National Science Laboratory (YerPhI),
2. Alikhanian Br. Street, 0036 Yerevan, Armenia.

Abstract

The role of neutron beam investigation is significant not only for fundamental science but also for various fields of applied science. This work is dedicated to the formation of neutron beams using the external 18-MeV proton beam of IBA cyclotron C18/18 with a beam current of up to 100 μA. The facility is located at the A. Alikhanyan National Science Laboratory (Yerevan Physics Institute). The possibility to obtain thermal or epithermal neutron beams using the external proton beam of the cyclotron is studied using Geant4 simulations. In this case, a quasimonoenergetic neutron source ^{9}Be (p, n)^{9}B reaction is chosen. As a result of the simulations, the optimal thickness of the ^{9}Be beryllium isotope target is determined. The induced neutron beam is accompanied by a gamma ray background. To decrease the number of accompanying gamma rays, the lead absorber is considered. As a method of separating neutrons from gamma rays, the pulse shape discrimination (PSD) technique is developed. This study shows the possibility of neutron-gamma PSD and its applicability using the EJ-299-33A plastic scintillator..

Keywords: neutron beam; neutron-gamma discrimination.

1. Introduction

Study of the formation of quasimonoenergetic neutron beams is of interest from both practical and scientific points of view. Nowadays, monoenergetic neutron beams are widely used in medicine. From the viewpoint of science, these neutron beams are important in the study of neutron-induced reactions in low-energy regions. Because neutron-induced activation cross sections govern the rate of production of isomers and radioactive isotopes, these cross sections are important when estimating the radiation levels and decay heat of materials that have been exposed to radiation fields with a strong neutron component [1].

However, neutrons are not purely monoenergetic; rather, they are associated with the continuum neutron spectrum. Therefore, energy-angular distribution information related to the neutron continuum is required for the design of neutron sources and facilities shielding. There is a small amount of experimental data for the neutron continuum above 10-MeV proton energies. Most data are available for the angular distribution at 0° [2].

Preexperimental simulations were done using Geant4 software [3]. Geant4 includes facilities for handling geometry, tracking, detector response, run management, visualization, and user interface. Preexperimental simulations give an advantage when finding optimal parameters for real physical experiments, which means less time needs to be spent on low-level details and attention can be concentrated on more important aspects of the experiment.

* Corresponding author. A. Alikhanyan National Science Laboratory, Yerevan, Armenia. E-mail: rave@mail.yerphi.am
☆ Peer review under responsibility of Tomsk Polytechnic University.
https://doi.org/10.18799/24056537/2019/2/247

To generate a high level of neutron production, the ^{9}Be beryllium (Be) isotope target was chosen. This choice simplifies the problem of target cooling during irradiation because of the high melting point of Be (1,287 °C). All reaction channels emitting neutrons in a ^{9}Be(p,x) many-body reaction were considered in Geant4 simulations.

A special technique was developed to separate neutrons from accompanying gamma rays. A neutron detection system with a plastic scintillator was constructed and connected to the ultrafast oscilloscope available at the A. Alikhanyan National Science Laboratory (Yerevan Physics Institute).

The main goal of this study is to perform neutron-gamma discrimination. In the first part of this paper, the transformation of a proton beam into a neutron is described. The next section explains the separation of the neutrons from gamma rays by PSD. In the final section, the experimental procedure is described.

2. Neutron flux

^{7}Li(p,n) and ^{9}Be(p,n) reactions are used widely as quasimonoenergetic neutron sources [2]. In particular, the ^{7}Li(p,n) reaction is expressed as a monoenergetic peak in the 3- to 5-MeV region, and approximately half of the yield of this reaction is concentrated in the region up to 14 MeV. However, the low melting point of lithium (Li, 180.54 °C) compared with the melting point of Be (1,287 °C) requires an additional cooling system, which complicates the use of Li as a target [4].

As an intense source of neutrons, the ^{9}Be thick target through the (p,n) reaction is considered for applications because of its high neutron yields and good thermal conductivity [5, 6]. The target is described as "thick" when the proton beam is fully stopped inside of it. Basically, in applications, it is used for thermal and epithermal energy neutron beams. To reach the epithermal energy range of the generated neutrons, the beam shaping assembly (BSA) was used. Thermal and fast neutron components of the neutron beam, as well as the dose of gamma rays, will reduce the acceptable values. Simulations have shown [7] that the neutron yield was the highest in the thick target (^{9}Be target thickness was 2.5 mm).

Construction of a BSA is important to produce an intensive thermal neutron beam. Design and optimization characteristics of the BSA for neutron flux from a thick target were simulated by Geant4. Appropriate materials for the moderator and the reflector with optimal thicknesses were determined to obtain the thermal or epithermal neutron beams. Creation of the optimal BSA by Geant4 simulations gives the possibility increase the neutron flux in the thermal or epithermal neutron energy region [7].

The 18-MeV external proton beam, before reaching the target, passed through 500-μm aluminum foil, which was installed to sustain the vacuum inside the tube. Passing through the aluminum foil, the proton beam energy decreased up to 14.8 MeV.

The ^{9}Be(p,n)^{9}B two-particle reaction was accompanied by many-particle ^{9}Be(p,xn) reactions. In Table 1, all ^{9}Be(p,xn) reactions from energy thresholds up to 14.8 MeV are listed.

Table 1. ^{9}Be(p,xn) many-particle reactions up to 14.8-MeV thresholds

Reaction	Q Value (MeV)	Energy Threshold (MeV)
$p + {}^{9}\mathrm{Be} \rightarrow {}^{9}\mathrm{B} + n$	–1.8504	2.0572
$p + {}^{9}\mathrm{Be} \rightarrow {}^{9}\mathrm{B} + n + \gamma$	–1.8855	2.057
$p + {}^{9}\mathrm{Be} \rightarrow {}^{8}\mathrm{Be} + p + n$	–1.6645	1.8507
$p + {}^{9}\mathrm{Be} \rightarrow {}^{8}\mathrm{Be} + p + n + \gamma$	–1.7011	1.8507
$p + {}^{9}\mathrm{Be} \rightarrow {}^{5}\mathrm{Li} + \alpha + n + \gamma$	–3.5377	3.9333
$p + {}^{9}\mathrm{Be} \rightarrow 2\alpha + p + n$	–1.5727	1.74859

From Table 1, along with neutrons, accompanying γ, p, α, and different nuclei are formed during the reaction. The neutron-charged particle separation was relatively easy (magnetic fields can be used) compared with that of neutral particles. The most difficult challenge was neutron-gamma ray separation because of lack of reaction to the magnetic fields.

Fig. 1 shows the neutron and gamma ray energy spectra from ^{9}Be(p,xn) reactions.

Based on Geant4 simulations [7], the best option to decrease associated gamma ray yield compared with neutrons was determined. The system consists of the ^{9}Be 2.5-mm target and 1.27-cm lead sheet. Table 2 lists the summary of Geant4 simulation results of the neutron-to-gamma ray ratio for the 2.5-mm Be target and different thicknesses of lead sheets.

Table 2. Neutron-to-gamma ray ratio for different thicknesses of lead sheets installed after 2.5-mm Be target

Thickness of Lead (cm)	0	0.5	1.27
$N_{\mathrm{neutrons}}/N_{\mathrm{gamma}}$	0.55	0.99	1.35

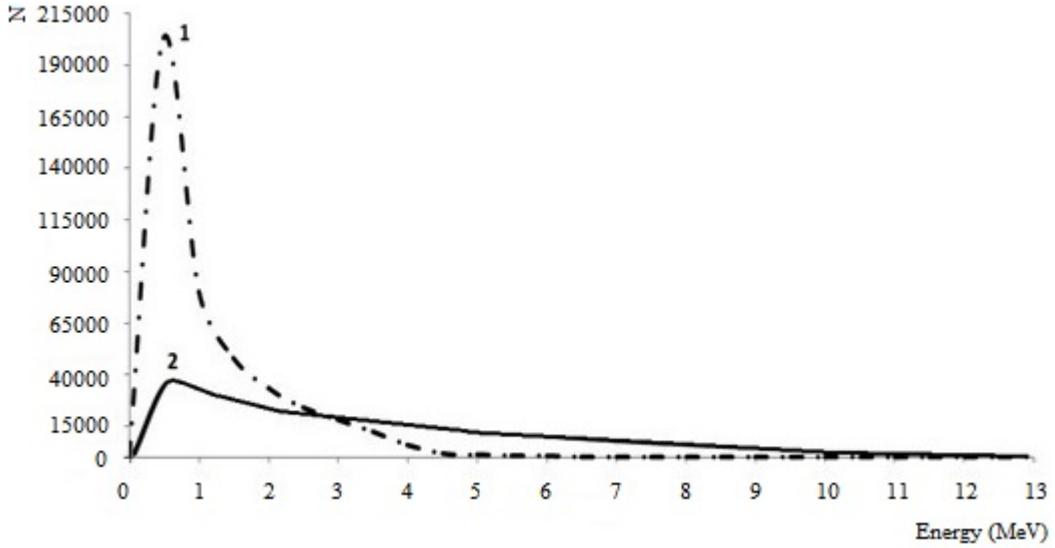

Fig. 1. Energy spectra of gamma rays (1) and neutrons (2) for 2.5-mm ^{9}Be target

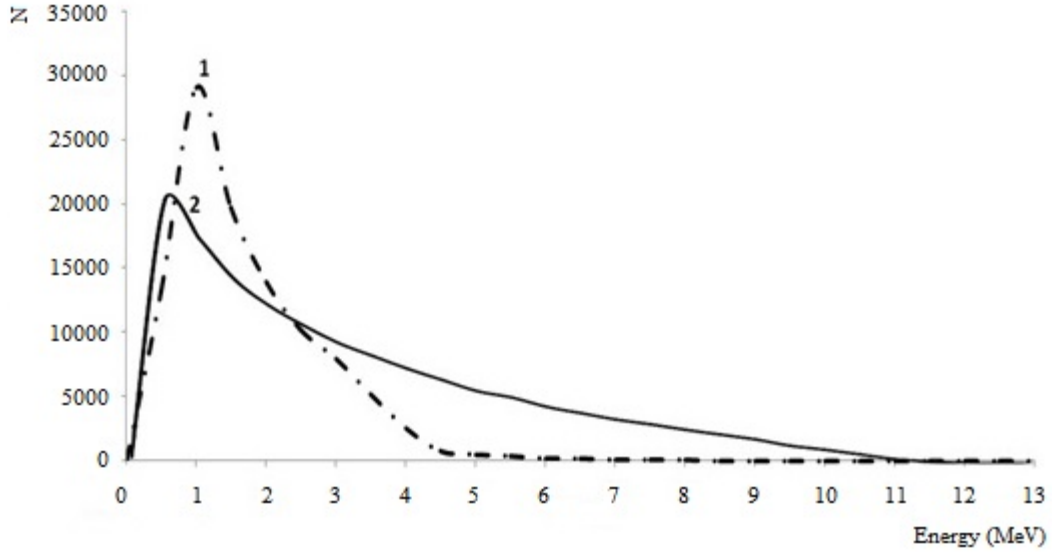

Fig. 2. Energy spectra of gamma rays (1) and neutrons (2) for 2.5-mm Be target and 1.27-cm lead sheet

The neutron-to-gamma ray spectra for the previously mentioned optimal size of the lead sheet are shown in Fig. 2.

During an experiment on IBA cyclotron C18/18, the time-of-flight technique was used [8, 9] to detect neutrons. To develop the neutron-gamma discrimination methodology, the ^{252}Cf californium isotope ($T_{1/2}$ = 2.645 y) neutron source was used.

The ^{252}Cf neutron source is widely used for spontaneous fission. It is also used as a small neutron source. ^{252}Cf decays into the ^{248}Cm curium isotope through α decay ($T_{1/2}$ = 2.645 y). This process is accompanied by evaporation of neutrons. Fission neutrons of ^{252}Cf have energy up to 13 MeV, with a middle value of 2.3 MeV and a most probable value of 1 MeV. These secondary fragments are usually in excited states and promptly emit gamma rays, which go along with neutrons.

3. Neutron-gamma discrimination

The main challenge of fast neutron detection is to dissociate neutron response from the gamma ray background. Unlike alpha or beta rays, neutrons have a scintillator penetration range similar to that of gamma rays. Only the ionization mechanism is slightly different, which can produce some kind of signal discrepancy. PSD was chosen to observe, separate, and attribute individual emissions from a neutron or a gamma ray [10]. The most widely used method for high-energy neutron detection in the presence of a gamma radiation background uses the difference in the shapes of the scintillation pulses excited by neutrons and gamma rays in organic scintillators.

PSD was discovered and demonstrated a few decades ago [11]. It is based on the existence of two-decay component fluorescence. The essence of this

phenomenon is that in addition to the main component decaying exponentially (prompt fluorescence), usually there is a slower emission that has the same wavelength but a longer decay time [12].

In this work, the research processes of nuclear physics and high-energy particle physics and the utilization of digital technology to separate the scintillation responses of neutrons and photons in experimental installations are suggested. One of the ways to separate neutrons from gamma rays is to analyze the pulse shape from the photomultiplier (PMT). It is known that amplitudes of neutrons and gammas at the same pulse have different tail lengths. The integral area of the pulse in comparison with the partial area can give information about the origin of the pulse. Neutron-generated pulses have long tails, and with this information, they can be separated from gamma-generated pulses with prompt signals.

The experimental setup intended for the development of the technique consisted of the following elements: EJ-299-33A, a solid-state plastic scintillator manufactured by Eljen Technologies [13]; a Thorn EMI electronics tube 9954A PMT [14]; the DAQ-PicoScope 5000 Series manufactured by Pico Technology [15]; and ^{252}Cf as a neutron source.

The EJ-299-33A pulse shape discrimination (PSD) plastic scintillator enables the separation of gamma and fast neutron signals based on their timing characteristics. The scintillator is stable in water, dilute acids, and alkalis, lower alcohols, and silicone greases. It can be used safely with most epoxies and glues. Plastic scintillators typically consist of a solid solution of organic scintillating molecules in a polymerized solvent. Because of the ease with which they can be shaped and fabricated, plastic scintillators have become an extremely useful form of organic scintillator. They exhibit several advantages over their liquid counterparts, such as increased durability, and flexibility in manufacturing detectors of various sizes and shapes. They are nontoxic and nonflammable, which makes plastic scintillators safer in usage than liquid scintillators. The relatively low cost of plastic makes it an economical choice for applications for which large-volume scintillators are required (for example, inspecting cargo containers in shipping ports or trucks at border crossings). The high hydrogen content makes them ideal for use in the detection of high-energy neutrons. Furthermore, plastic scintillators have a demonstrated capability for PSD. Properties for the EJ-299-33A plastic scintillator are presented in Table 3 [16].

Table 3. Properties of EJ-299-33A solid-state plastic scintillator

Properties	EJ-299-33A
Light output (% anthracene)	56
Scintillation efficiency (photons/1 MeV e^-)	8,600
Wavelength of maximum emission (nm)	425
H atoms (no. per cm^3)	5.13×10^{22}
C atoms (no. per cm^3)	4.86×10^{22}
Electrons (no. per cm^3)	3.55×10^{23}
Density (g/cm^3)	1.08

The Thorn EMI 9954A PMT is a 51-mm-diameter (2-inch-diameter) end window PMT, with an enhanced green-sensitive bialkali photocathode and 12 Be-copper dynodes of linear-focused design for good linearity and timing.

The PicoScope 5000 Series of flexible resolution oscilloscopes from Pico Technology constitute a range of high-specification, real-time measuring instruments that connect (**s**) to the USB port of a computer. They use the PicoScope software to work as oscilloscopes and spectrum analyzers. With various options of portability, resolution, deep memory, fast sampling rates, and high bandwidth, these highly versatile oscilloscopes suit a range of applications.

4. Experimental procedure

To select the supply voltage and the discrimination threshold, as well as cut off the noise pulses of the PMT, the background counting characteristic of the PMT at different voltage values was investigated. The measurements were taken using the assembled detector. The ^{252}Cf neutron source with activity of 1 μCi was used. The measurements were performed for the following three cases:

1. Background without the ^{252}Cf source
2. With the ^{252}Cf source, a detector-source distance of 2 cm
3. ^{252}Cf source with a lead absorber

Then, 10,000 events were collected from the neutron source and analyzed by pulse shape analysis and pulse shape identification software for all cases mentioned earlier.

The received data were processed by a dedicated application written in the ROOT framework. In each case, the application identified a peak on the pulse shape, shifted it by 3 ns, and then registered the amplitude at that point (called the edge). Because the pulse durations are different at the same energies of

neutrons and photons, the tail of the neutrons will be longer than the tail of the photons. Thus, the ratio of the edge to the peak amplitude of the neutron will be higher than that of the photon.

5. Results and discussion

In Fig. 3, the total area of the pulse to the amplitude is shown. The smaller inclination to the X axis corresponds to the photons, because at the same amplitude, the pulse area is smaller than it is for the neutrons.

In Fig. 4, the neutron-gamma discrimination is illustrated. The peak near zero corresponds to the events of the background and gamma rays. The distribution near 0.8 corresponds to the neutron peak.

The small value of the peak results from the low intensity of the ^{252}Cf. If a cyclotron's proton beam is used as the source of the neutron beam, the neutron beam intensity will be higher.

Conclusion

The yield of neutrons based on the ^{9}Be(*p*,*xn*) reaction on the external proton beam of cyclotron C18/18 has been calculated using Geant4. The neutron beam can be used for different applications, applied sciences, and fundamental research.

The technique for high-energy neutron detection in the presence of gamma background has been developed. The suggested method provides an opportunity to reliably separate neutrons from accompanying gamma rays during experiments on cyclotron C18/18. In addition, it is intended for continued investigations with a more powerful neutron source to determine the best results. In the future, this method will be used for detection of the obtained neutrons from the extracted proton beam of cyclotron C18/18.

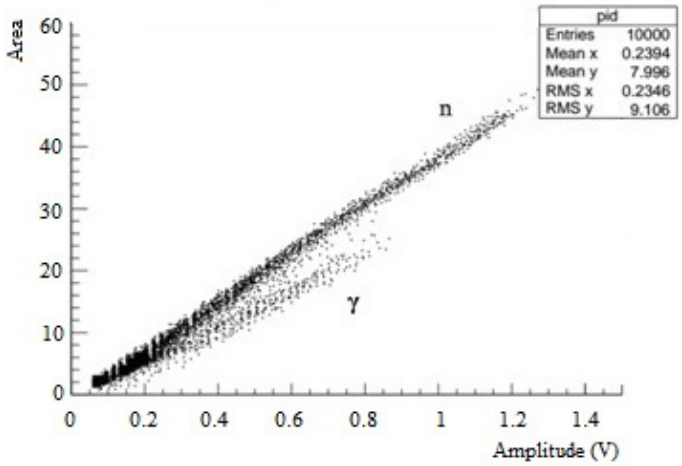

Fig. 3. Dependence of total area of pulse on amplitude

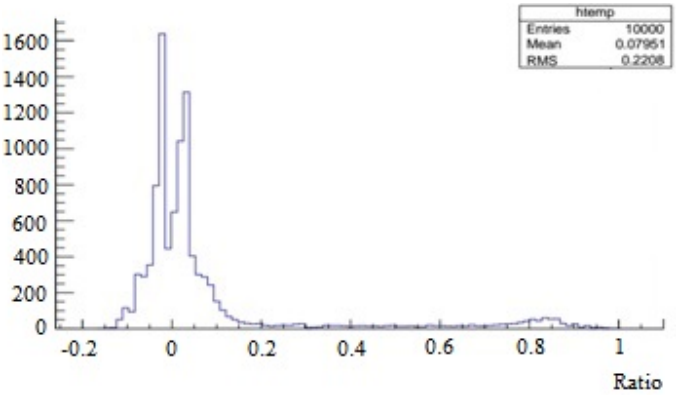

Fig. 4. Neutron-gamma discrimination

References

[1] Plompen A., Chadwick M.B., Koning A.J. International Evaluation Co-operation, Neutron activation cross-section measurements from threshold to 20 MeV for the validation of nuclear models and their parameters. France, Nuclear Energy Agency, Organisation for Economic Co-operation and Development, 2005, 256 p.

[2] Kamada S., Itoga T., Unno Y., Takahashi W., Oishi T., Baba M. Measurement of Energy-angular Neutron Distribution for ^{7}Li, ^{9}Be(p,xn) Reaction at E_P = 70 MeV and 11 MeV. *Journal of the Korean Physical Society*, 2011, vol. 59, no. 2, pp. 1676–1680. doi: 10.3938/jkps.59.1676.

[3] Agostinelli S., *et al.* GEANT$_4$-A simulation toolkit. *Nuclear Instruments and Methods in Physics Research Section A,* 2003, vol. 506, no. 3, pp. 250–303. doi: 10.1016/S0168-9002(03)01368-8.

[4] Avetisyan R., Avagyan R., *et al.* Neutron-induced reactions investigations in the neutrons energy range up to 16 MeV. *Proceedings of the 33rd International Workshop on Nuclear Theory*, 2014, vol. 33, pp. 172–178.

[5] Lavelle C.M., *et al.* Neutronic design and measured performance of the Low Energy Neutron Source (LENS) target moderator reflector assembly. *Nuclear Instruments and Methods in Physics Research Section A*, 2008, vol. 587, no. 2–3, pp. 324–341. doi: 10.1016/j.nima.2007.12.044.

[6] Mattera A., *et al*. Characterization of a Be(p,xn) neutron source for fission yields measurements. *Proceedings of the International Conference on Nuclear Data for Science and Technology*, 2013, pp. 1–3.

[7] Avagyan R., Avetisyan R., Ivanyan V., Kerobyan I. Study of low energy neutron beam formation based on GEANT4 simulations. *Nuclear Instruments and Methods in Physics Research B,* 2017, vol. 402, pp. 247–250. doi: 10.1016/j.nimb.2017.03.091.

[8] Iwamoto Y., *et al*. Measurements of double-differential neutron-production cross-sections for the ^{9}Be(p,xn) and ^{9}Be(d,xn) reactions at 10 MeV. *Nuclear Instruments*

and Methods in Physics Research Section A, 2009, vol. 598, no. 3, pp. 687–695. doi: 10.1016/j.nima.2008.10.019.

[9] Hagiwara M., *et al.* Spectrum Measurement of Neutrons and Gamma-rays from Thick H182 O Target Bombarded with 18 MeV Protons. *Journal of the Korean Physical Society,* 2011, vol. 59, no. 23, pp.2035–2038. doi:10.3938/jkps.59.2035.

[10] Bertrand G.H.V., Hamel M., Normand S., Sguerra F. Pulse shape discrimination between (fast or thermal) neutrons and gamma rays with plastic scintillators: State of the art. *Nuclear Instruments and Methods in Physics Research A,* 2015, vol. 776, pp. 114–128. doi: 10.1016/j.nima.2014.12.024.

[11] Brooks F.D. A scintillator counter with neutron and gamma-ray discrimination. *Nuclear Instruments and Methods*, 1959, vol. 4, no. 3, pp. 151–163. doi: 10.1016/0029-554X(59)90067-9.

[12] Zaitseva N., Glenn A., *et al.* Pulse shape discrimination in impure and mixed single-crystal organic scintillators. *IEEE Transactions on Nuclear Science*, 2011, vol. 58, no. 6 part 2, pp. 3411–3420. doi: 10.1109/TNS.2011.2171363.

[13] EljenTechnology, EJ-299-33. Available at: http://www.eljnetechnology.com/index.php/products/plastic-scintillators/114-ej-299-33.

[14] ET Enterprises, Electron tubes. Available at: http://et-enterprises.com/images/data_sheets/9954B.pdf.

[15] PicoScope 5000 A and B Flexible Resolution Oscilloscopes. User's Guide. Available at: https://www.picotech.com/download/manuals/picoscope-5000-a-and-b-series-users-guide.pdf.

[16] Hartman J., Barzilov A., Peters E.E., Yates S.W. Measurements of response functions of ej-299-33a plastic scintillator for fast neutrons. *Nuclear Instruments and Methods in Physics Research A,* 2015, vol.804, pp. 137–143. doi: 10.1016/j.nima.2015.09.068.

Received: 22.11.2018